

A Systematic Study of the Synthesis of Silver Nanoplates: Is Citrate a “Magic” Reagent?

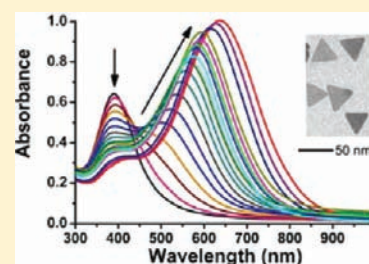
Qiao Zhang,[†] Na Li,^{†,‡} James Goebel,[†] Zhenda Lu,[†] and Yadong Yin^{*,†}

[†]Department of Chemistry, University of California, Riverside, California 92521, United States

[‡]School of Chemical Engineering and Technology, Harbin Institute of Technology, Harbin, Heilongjiang 150001 P.R. China

S Supporting Information

ABSTRACT: In this work we have carried out systematic studies and identified the critical role of hydrogen peroxide instead of the generally believed citrate in the well-known chemical reduction route to silver nanoplates. This improved understanding allows us to develop consistently reproducible processes for the synthesis of nanoplates with high efficiency and yields. By harnessing the oxidative power of H₂O₂, various silver sources including silver salts and metallic silver can be directly converted to nanoplates with the assistance of an appropriate capping ligand, thus significantly enhancing the reproducibility of the synthesis. Contrary to the previous conclusion that citrate is the key component, we have determined that the group of ligands with selective adhesion to Ag (111) facets can be expanded to many di- and tricarboxylate compounds whose two nearest carboxylate groups are separated by two or three carbon atoms. We have also found that the widely used secondary ligand polyvinylpyrrolidone can be replaced by many hydroxyl group-containing compounds or even removed entirely while still producing nanoplates of excellent uniformity and stability. In addition to the general understanding of NaBH₄ as a reducing agent, it has also been found to act as a capping agent to stabilize the silver nanoparticles, prolong the initiation time required for nanoplate nucleation, and contribute to the control of the thickness as well as the aspect ratio of silver nanoplates. The improved insight into the specific roles of the reaction components and significantly enhanced reproducibility are expected to help elucidate the formation mechanism of this interesting nanostructure.



INTRODUCTION

Silver nanoplates, also referred to as nanoprisms or nanodisks, are two-dimensional plasmonic nanostructures that have attracted intensive attention due to their strong shape-dependent optical properties and related applications.^{1–5} When the lateral dimension of silver nanoplates is much larger than the thickness, they possess an extreme degree of anisotropy, which favors a high tunability of their localized surface plasmon resonance (LSPR) and therefore generates maximum electromagnetic-field enhancement.⁶ After the seminal report by Mirkin et al. on the photo-induced synthesis of silver nanoplates in 2001,⁷ a variety of solution-based strategies have been developed by many other groups to synthesize silver nanoplates, including photochemical processes,^{8–13} ligand-assisted chemical reductions,^{14–16} electrochemical synthesis,¹⁷ templating procedures,¹⁸ and sonochemical routes.¹⁹ Among all these methods, direct chemical reduction has been the most popular due to the considerably high yield and relatively simple setups and procedures which show promise for large-scale production.^{20–25}

The formation of extremely anisotropic silver nanoplates is not thermodynamically favored because it involves a competition against the desire to minimize the surface area and energy through the formation of Wulff polyhedrons (a truncated octahedron) enclosed by a mix of {111} and {100} facets.^{26–28} Much effort has been made to understand the mechanism, and many hypotheses have been proposed to explain the formation of such

highly anisotropic structures. The most popular theory at the early stages of research was the “face-blocking theory”, in which a capping agent selectively adheres to a particular crystal facet of the growing nanocrystal and thus slows the growth rate of that facet relative to the others.^{1,2} However, it has been gradually realized that preferential anisotropic growth is dependent not only upon the selective adhesion of capping ligands but also on the crystal symmetry of the starting nuclei.^{21,29} For materials with isotropic crystal structures, anisotropic growth cannot be guaranteed by simply introducing selective binding ligands into the reaction. Instead, it is usually facilitated by breaking the isotropic symmetry with the formation of twin or other defect planes during the nucleation stage, which is, however, still a great challenge to control during synthesis. Based on crystallographic arguments, it is believed that the final morphology of the nanostructure is determined by the internal crystal structure of the original seed particle because of the limited number and variety of crystal facets available for growth.^{30–32} Pileni et al. have attributed the 1/3{422} reflections observed in silver and gold nanoplates, which should be forbidden for a perfect fcc structure, to parallel stacking faults in the <111> direction,³³ and further pointed out that these stacking faults should be responsible for the formation of plate structures by providing low-energy

Received: August 25, 2011

Published: October 14, 2011

reentrant grooves which energetically favor lateral crystal growth. The fact that plate structures are more often observed in silver and gold than other metals is due to their lowest stacking fault energies.²⁷ On the basis of high-resolution transmission electron microscopy (HRTEM) and X-ray diffraction (XRD) studies, Rocha and Zanchet found that the internal structure of silver nanoplates is indeed very complex, containing many twins and stacking faults.³⁴ In their studies, planar defects in the $\langle 111 \rangle$ direction have been found to give rise to local hcp regions, which can also be used to explain the existence of forbidden 2.50 Å fringes that are observed in $\langle 111 \rangle$ orientated nanoplates. Kelly et al. further elucidated the formation mechanism of the hcp layer which was used to explain the evolution of silver nanoplates.³⁵ Xia et al. have recently pointed out the importance of interweaving both crystallographic and surface chemistry arguments in order to discern the overall mechanism of nanoplate formation.^{4,36}

Despite the continuously improving understanding of the cause of plate formation by defects, the chemical origin of these defects has remained largely unknown. This is mainly due to the lack of systematic studies to clarify the role of each reagent in determining the structure of seeds and their growth process, which often leads to contradictory conclusions that make it difficult to ascertain the true cause of defect formation. For example, while many prior works have deemed some chemicals such as citrate and/or polyvinylpyrrolidone (PVP) to be critically important components in a given reaction, a number of researchers have attributed their success in nanoplate synthesis to the presence of other chemical species or reaction conditions.³⁴ In addition, other researchers have demonstrated the production of silver nanostructures with different morphologies by starting with the same seeds but under slightly altered synthetic conditions, such as seed concentration, surfactants, pH value, and reaction temperature.² The lack of deep understanding of the specific contributions of the reaction components also makes it difficult to reproduce many of the reported results with satisfactory yield and quality because some minor unintentional alterations to the reaction conditions may easily disturb nanoplate formation.

In this paper, we reveal the specific roles of each reagent in the chemical reduction route to silver nanoplates through a comprehensive study. This significantly refined understanding allows us to develop an efficient and highly reproducible process for producing silver nanoplates with controllable edge length and thickness as well as desired surface plasmon resonance bands. We find hydrogen peroxide (H_2O_2), an oxidative etchant, to be the most essential component, which helps to induce the formation of planar twinned seeds, remove possible nontwinned particles, and eventually produce silver nanoplates with high yields. Contrary to previous reports in which citrate is considered to be a “magic” component critically required for the formation of silver nanoplates, our investigation clearly points out, for the first time, that citrate is not an irreplaceable component: it is required to stabilize the formed silver nanoplate nuclei through preferential binding to the (111) facets but can be completely substituted by many other carboxyl compounds containing two carboxylate groups. The preferential binding affinity of such carboxyl compounds seems to come from the two nearest carboxylate groups, which are separated from each other by two or three carbon atoms. This is a different conclusion from the one suggested in previous theoretical simulations.³⁷ Many prior works have also claimed the importance of the coexistence of two capping ligands, typically citrate and PVP, in the formation of silver nanoplates.²⁰

In this study, however, we find that a single carboxylate ligand is sufficient to obtain high-quality silver nanoplates in a stable colloidal form. The exclusion of PVP not only simplifies the reaction but also improves the reproducibility of the synthesis. All of these features are beneficial for large-scale synthesis and future practical applications. Furthermore, the silver source has been found to be the least critical factor in this reaction: many forms of silver, including silver salts and metallic silver particles, can be used to produce nanoplates of similar good quality and yield, as long as there is a sufficient amount of H_2O_2 in the system to ensure that the silver is in cationic form before reduction occurs. In addition to the general understanding that NaBH_4 is a reducing agent, we found its surprising secondary role as a capping agent which can stabilize the Ag nanoparticles, as evidenced by the prolonged initiation time required for nucleation at a higher concentration of NaBH_4 . In a broader sense, we want to use the results obtained in this work to point out the importance of systematic studies in general nanostructure synthesis: they help to identify the appropriate reaction “window” through the determination of the most critical reaction conditions. Many difficult syntheses, which may originally appear challenging to reproduce as the conditions are often located at the edge of the reaction window, can be significantly improved in their reproducibility by moving the conditions to the center of this window in which small interferences will not significantly change the quality and yield of the products. The key to a highly reproducible synthesis is therefore to identify the most critical components and understand their contributions to the nanostructure evolution.

EXPERIMENTAL SECTION

Chemicals. Hydrogen peroxide (H_2O_2 , 30 wt-%), acetic acid (glacial), sodium hydroxide, and sodium potassium tartrate were purchased from Fisher Scientific. Silver nitrate (AgNO_3 , 99+%), sodium borohydride (NaBH_4 , 99%), ethylene glycol (EG), sodium citrate tribasic dihydrate (TSC, 99%), tricarballic acid (99%), and L-ascorbic acid were obtained from Sigma-Aldrich. Polyvinylpyrrolidone (PVP, $M_w \approx 29,000$) was purchased from Fluka. Malonic acid disodium salt monohydrate (99%), succinic acid disodium anhydrous (99%), glutaric acid (99%), oxalic acid (98%), DL-isocitric acid trisodium hydrate (98%), 1,3,5-benzenetricarboxylic acid (98%), pimelic acid (98%), and polyethylene glycol (PEG, $M_w \approx 3500$) were purchased from Acros Organics. Adipic acid disodium salt was purchased from TCI America. Diethylene glycol (DEG) was purchased from Alfa Aesar. All chemicals were used as received without further treatment.

Synthesis of Ag Nanoplates. In a standard synthetic approach, the total volume of the reaction solution is fixed at 25.00 mL. Typically, a 24.75 mL aqueous solution combining silver nitrate (0.05 M, 50 μL), trisodium citrate (75 mM, 0.5 mL), and H_2O_2 (30 wt %, 60 μL) was vigorously stirred at room temperature in air. Sodium borohydride (NaBH_4 , 100 mM, 250 μL) was rapidly injected into this mixture to initiate the reduction, immediately leading to a light-yellow solution. After ~ 3 min, the colloidal solution turned to a deep yellow due to the formation of small silver nanoparticles. Within the next several seconds, the morphology started to change from particles to nanoplates accompanied by the solution color changing from deep yellow to red, green, and blue. The entire transition from nanoparticle to nanoplates typically took 2–3 min. In some reactions, poly(vinylpyrrolidone) (PVP, weight-average molecular weight $M_w \approx 29,000$ g/mol, 17.5 mM, 0.1 mL) was added to the original reaction mixture to narrow the plate size distribution and enhance their stability. In the presence of PVP, the transition from light yellow to deep yellow took ~ 30 min to occur. For the other

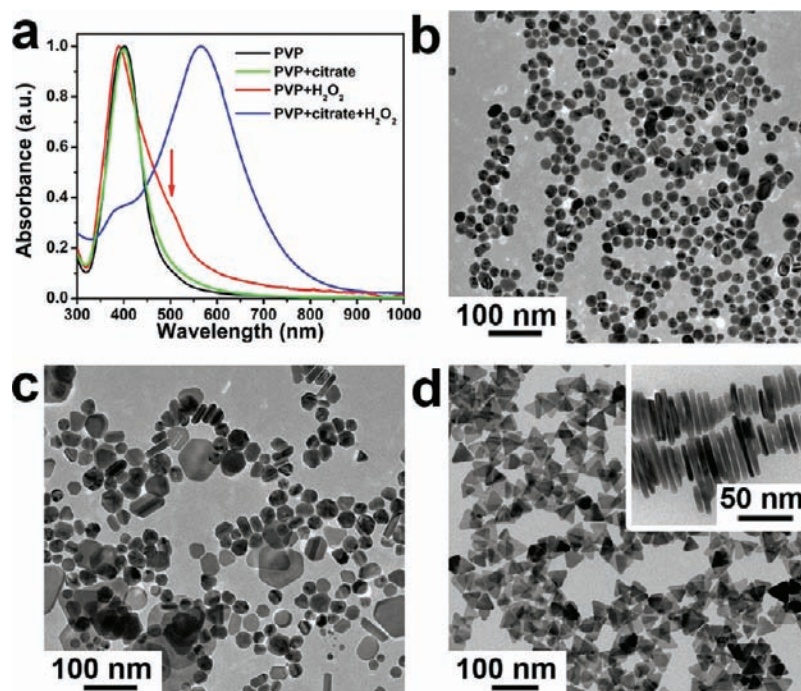


Figure 1. (a) UV/vis spectra of silver nanoparticles synthesized in different conditions; (b–d) TEM images showing the morphology of products prepared in the presence of (b) PVP only, (c) PVP and H_2O_2 , and (d) PVP, citrate, and H_2O_2 together. The inset in (d) shows a TEM image in which Ag nanoplates stand vertically upon their edges.

specific conditions, e.g., different surfactants or concentrations, the synthetic procedures are described in the figure captions in the Supporting Information.

Characterization. The morphology of Ag nanoparticles was characterized by using a Tecnai T12 transmission electron microscope (TEM). The measurement of optical property was conducted by using a Varian Cary 50 UV/vis spectrophotometer (190 nm – 1100 nm). A probe-type Ocean Optics HR2000CG-UV-NIR spectrometer was used to measure the UV–vis spectra of the reaction system to obtain the real-time spectra change during the synthesis of silver nanoplates.

RESULTS AND DISCUSSION

In the direct chemical reduction scheme, Ag nanoplates are typically prepared by reducing an aqueous solution of AgNO_3 with NaBH_4 in the presence of trisodium citrate (TSC), PVP, and H_2O_2 .^{20,21,38} To investigate the specific roles of each reagent in this system, we start from a simple reduction reaction by simply mixing the silver source AgNO_3 and the reducing agent NaBH_4 . Under magnetic stirring, the solution changed color from light yellow to brownish in about 3 min. The brownish color came from large aggregations of silver nanoparticles due to the absence of stabilizer. When PVP and citrate were added either separately or combined, the reactions produced quasi-spherical silver nanoparticles which displayed a sharp plasmon peak at around 400 nm in the extinction spectra (Figure 1). This phenomenon confirms the stabilizing effect of these ligands but rules out their immediate shape-directing effect. In contrast, when a small amount of H_2O_2 was added together with PVP to the reaction, a shoulder around 500 nm appeared, implying the formation of some anisotropic nanoparticles. As evidenced by the TEM image shown in Figure 1c, the as-obtained product was a mixture of spherical and rod- and plate-like nanoparticles with a

nanoplate yield of $\sim 10\%$. These results clearly suggest that H_2O_2 can promote the formation of anisotropic structures. When citrate, PVP and H_2O_2 were added with an appropriate ratio into the reaction, Ag nanoplates with high yield and great uniformity can be obtained, as shown in Figure 1d. Such silver nanoplates tend to stack upon each other face-to-face and stand vertically on their edges, making it convenient to estimate their thicknesses (inset in Figure 1d). As we will discuss in more detail later, the combination of H_2O_2 and citrate at the appropriate ratio can also produce silver nanoplates of similar quality and yield, suggesting that PVP is nonessential to the formation of silver nanoplates.

As H_2O_2 appears to be the most critical reagent for the plate formation, we have studied its role more systematically. To simplify the reaction, we prepared silver nanoplates in the presence of citrate but without PVP under the typical conditions described in the Experimental Section. Without the addition of H_2O_2 , only quasi-spherical silver nanoparticles can be obtained after about 3 min of reaction, as indicated by the yellow color of as-prepared colloids. When the concentration of H_2O_2 was increased to 5 mM, a sharp peak around 450 nm appeared along with a shoulder at around 400 nm (Figure 2a), suggesting the formation of both plate-like structures and spherical nanoparticles, which has also been confirmed by TEM characterization. The sharp characteristic peak of silver nanoparticles at ~ 400 nm disappeared as the concentration of H_2O_2 was increased to 10 mM. The weak shoulder around 380–420 nm can be attributed to the in-plane quadrupole resonance of silver nanoplates. When the concentration of H_2O_2 was further increased to 20 mM, the quadrupole resonance became more pronounced and the dipole resonance red-shifted to ~ 600 nm. To investigate the detailed formation process of the silver nanoplates, we monitored the change in the SPR peak during the

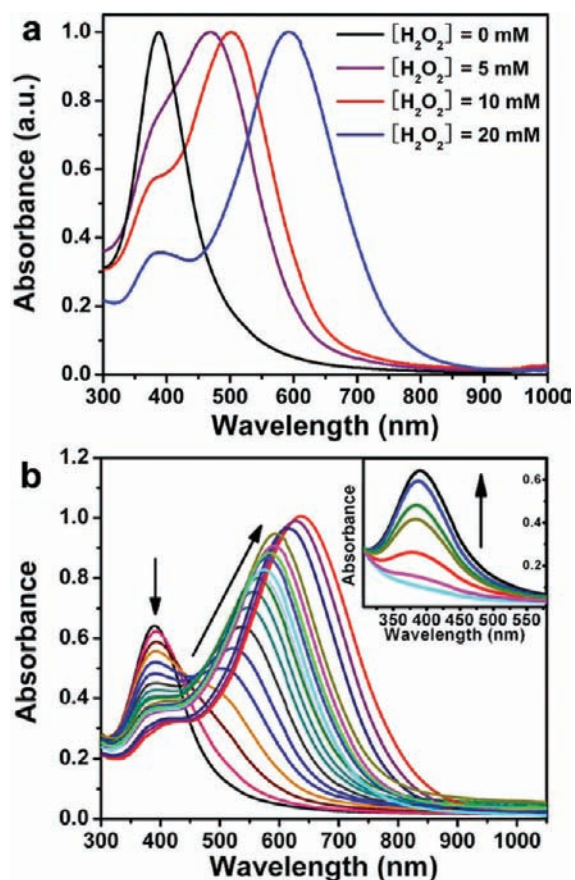
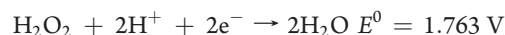


Figure 2. (a) UV/vis spectra of silver nanoparticles obtained by controlling the concentration of H_2O_2 ; (b) real-time measurement of the formation of silver nanoplates with a time interval of 7.5 s. The inset in (b) shows the UV/vis spectra of the initiation stage during the synthesis of silver nanoplates with a time interval of 0.75 s.

nucleation and growth of silver nanoplates under the standard conditions with 20 mM H_2O_2 . Upon the addition of NaBH_4 , the originally colorless solution became light yellow immediately, suggesting the reduction of silver. However, the characteristic peak of silver nanoparticles around 400 nm is not pronounced, as shown by the bottommost curve in the inset of Figure 2b. Instead, there is a very strong absorption band in the short UV range (<300 nm, not shown), implying the existence of small silver nanoparticles.^{39,40} After ~ 3 min of reaction, the light-yellow solution turned deep yellow in the span of several seconds, suggesting the formation of silver nanoparticles. The change in the optical property of the colloidal solution was recorded using a UV/vis spectrometer. As shown in the inset of Figure 2b, once the formation of nanoparticles began, the intensity of the characteristic peak at 400 nm increased quickly. In about 5 s, the peak rose to the maximum. The color of the reaction solution then quickly changed from deep yellow to red, green, and finally blue, as evidenced by the UV/vis spectra shown in Figure 2b. The intensity of the characteristic peak of spherical nanoparticles quickly decreased, indicating their consumption during the reaction. At the same time, another peak at ~ 500 nm emerged and gradually red-shifted to longer wavelengths, implying the formation and growth of silver nanoplates. The formation and development of silver nanoplates took about 2–3 min. A video showing the real time monitoring of the corresponding UV/vis spectrum is

provided in the Supporting Information. To further clarify the role of H_2O_2 , the reaction process in the absence of H_2O_2 has also been studied. Only a small peak at around 400 nm was noticeable in the UV/vis spectra, indicating the formation of large silver nanoparticles at the initial stage (Supporting Information).⁴¹

It is well-known that H_2O_2 is a powerful oxidizing agent.⁴² The standard potential in the peroxide–water couple is dependent on the pH value of the solution.^{43,44} In acidic solutions:



and in alkaline solutions:



Since the potentials under both conditions are higher than that of Ag^+/Ag ($E^0 = 0.7996 \text{ V}$), H_2O_2 can be used as an effective etchant to dissolve metallic silver. The results thus suggest that H_2O_2 acts as an oxidant from the very beginning of the reaction, and there should be a dynamic equilibrium between the reduction of silver ions by NaBH_4 and oxidative dissolution of metallic silver by H_2O_2 . On the basis of this understanding and the aforementioned experimental observations, we propose here a plausible mechanism for the formation of nanoplates: upon the injection of NaBH_4 , silver ions are partially reduced to form small silver nanoparticles, which are temporarily stabilized by the adsorption of citrate and borohydride ions. At the same time, extensive growth of the small nanoparticles to nanoplates is inhibited due to etching by H_2O_2 . As the result of dynamic equilibrium between the reduction and oxidation, silver stays in the form of small nanoparticles which appear light yellow in color. When NaBH_4 is consumed over time, the protection from borohydride ions is weakened, allowing the production of silver nuclei with various structures, as supported by the rise of a sharp peak around 400 nm (inset in Figure 2b). Due to the Ag–citrate coordinating interaction and the presence of the powerful etchant, H_2O_2 , the nuclei are silver nanoparticles containing many defects, including the twinned defects that favor the planar growth into plate shapes. Although it remains an interesting assumption for future exploration, we suspect that H_2O_2 can remove the relatively unstable nanoparticles at this stage, leaving only the most stable ones. With the protection of citrate ions that preferentially bind to (111) facets, plate-structured silver nuclei possess the highest relative stability because the majority of the surface is capped by ligands. Their expansion along the twin plane into high-aspect-ratio nanoplates is enhanced by the fast growth of side facets, typically (100). Therefore, the net effect of H_2O_2 in this reaction, in synergy with citrate ions, is to promote the nucleation of plates by removing less stable silver nanoparticles of other structures.

Understanding the deterministic role of H_2O_2 in plate formation allows us to replace other components in the synthesis. For example, we found it possible to use metallic silver, instead of silver salt, as the silver source for nanoplate synthesis. In their first successful preparation of silver nanoplates, Mirkin and co-workers converted silver nanospheres into triangular nanoplates through a photoinduced method.⁷ It was later pointed out that only small nanoparticles can be converted due to their lower redox potential, while larger nanoparticles did not work well in the photoconversion process.¹² Some other groups reported that silver nanoplates can also be prepared by thermally treating silver nanospheres in the presence of surfactants, typically citrate.¹⁵ However, until now, conversion was believed to be limited to

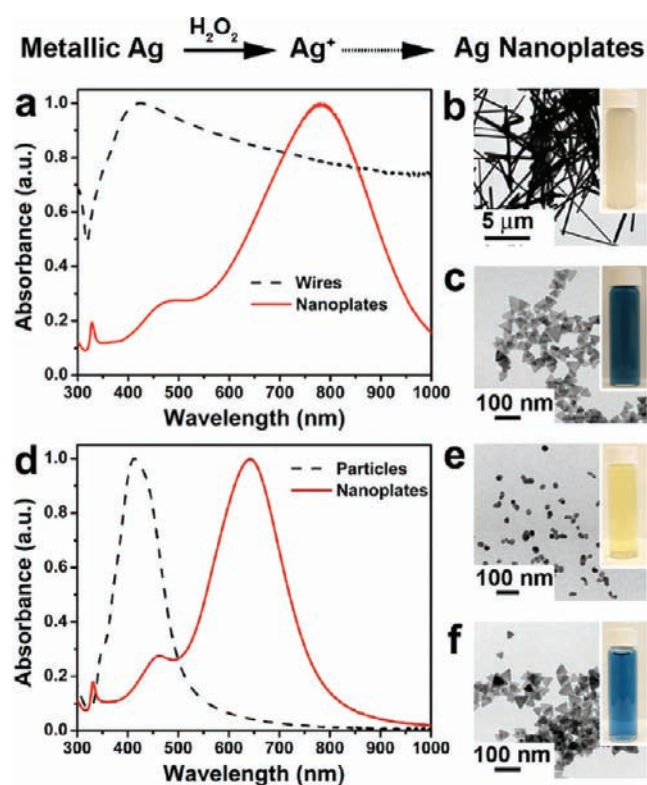


Figure 3. UV/vis spectra and TEM images showing that both (a–c) silver nanowires with lengths of up to 10 μm and (d–f) silver nanoparticles with irregular shapes can be converted to silver nanoplates in the presence of H_2O_2 .

small nanoparticles that are unstable under the specific reaction conditions. By using H_2O_2 as the etchant, we have found that all metallic silver particles, regardless of their size and shape, can be directly converted to silver nanoplates.

Figure 3 shows two examples of nanoplate synthesis by starting with preformed Ag nanowires and nanoparticles. In both cases, metallic silver is first dispersed in water, followed by the addition of citrate. Once a suitable amount of H_2O_2 has been added, the reaction solution gradually becomes colorless with the appearance of small bubbles due to the partial decomposition of H_2O_2 . NaBH_4 is then added to reduce Ag^+ back to Ag^0 . The solution changes gradually from colorless to light yellow, yellow, red, and blue, indicating the formation of silver nanoplates. As shown in a–c of Figure 3, silver nanowires with lengths of up to tens of micrometers can be converted to silver nanoplates, as confirmed by the UV/vis spectra and TEM images. During the conversion process, the original gray solution was changed to a dark blue solution. Another example is shown in d–f in Figure 3 in which irregular silver nanoparticles can be converted to silver nanoplates, which is supported by the corresponding UV/vis spectra and TEM characterization. The color change of the solution from bright yellow to blue also confirms the successful conversion. Additionally, these results rule out the possibility of an essential role for nitrate ions in the formation of silver nanoplates. From a synthesis point of view, the use of metallic silver as the source ensures a higher degree of reproducibility as there is less possibility of introducing disturbances such as the anions of the silver salt to the reaction.

Serving as a shape-directing agent and stabilizer, citrate has been widely used in the preparation of colloidal noble metal

nanoparticles, particularly Au and Ag.^{45,46} Since the first report on the synthesis of silver nanoplates,⁷ citrate has been considered an essential component. In the photochemical synthetic strategy, Xue and Mirkin found that citrate ion serves as a bifunctional reagent: not only can it reduce Ag^+ to Ag^0 in the presence of light irradiation, but it also helps to form plate-structured silver nanoparticles, although the mechanism was not discussed in more depth.¹² They also found that citrate was an essential component in the synthesis, which could not be replaced by other carboxyl compounds, such as tricarballoylate, citramalate, and aconitate. Isocitrate is the only other carboxyl molecule that was found to be able to replace citrate; however, the resulting yield and quality was considerably lower.¹² Although many groups have tried to determine the role of citrate,^{22,23,47} the nature of citrate ions in the formation of silver nanoplates is still unclear, which has made the citrate ion a “magic” ligand. It is widely accepted that citrate acts as a capping agent as it can selectively bind to {111} facets and thus effectively block the growth along the vertical axis and only allow extensive growth along the lateral direction.¹⁵ Consistent with this assumption, Kiline and Xia et al. pointed out that, theoretically citric acid can preferentially bind to Ag (111) facets due to the fact that the approximate three-fold symmetry of citric acid matches that of Ag (111) and results in four Ag–O bonds, while it forms only two bonds with Ag (100) because of the geometry mismatch.³⁷ Unfortunately, no prediction was given regarding whether any other molecules could play the same role in the synthesis of silver nanoplates. Since we have determined that the key in the synthesis of silver nanoplates is the formation of plate-structured nuclei in the presence of hydrogen peroxide, we are now able to systematically vary the capping ligands and study their contribution to plate formation.

Table 1 lists carboxyl compounds that have been used to prepare silver nanoplates in our study and the corresponding yields. It is unsurprising that no silver nanoplates could be obtained when acetate was used as a substitute for citrate since there was no geometric difference in its binding affinity to (111) or (100) facets. We then tested the use of dicarboxyl compounds as capping agents. Although oxalate has two carboxylate groups, no nanoplates were formed when it was used to replace citrate, which might be attributed to the size mismatch between the molecule and the atoms on the Ag (111) surface.³⁷ Surprisingly, many other dicarboxyl molecules can be used to replace citrate and yield a relatively high percentage of plate structures. For example, in the presence of malonate, a red colloid can be obtained, as evidenced by a sharp peak around 500 nm. TEM characterization also confirms the formation of silver nanoplates with a yield of $\sim 80\%$. When succinate and citramalate were used as the capping agents, silver nanoplates could be achieved with a yield of 100%. To further investigate the role of such carboxyl molecules, we also used long-chain carboxyl compounds as substitutes for citrate. As depicted in Figure 4, the yield of silver nanoplates is highly sensitive to the chain length of the capping agent. As the number of carbon atoms between the two nearest carboxylate groups increases beyond 2, the yield of silver nanoplates gradually drops. On the basis of Kiline and co-workers’ simulation, the two side methylene–carboxylate groups of citrate were found to bind to (111) facets, while the closer carboxyl group does not directly bind to the surface. If this conclusion is correct, the ideal number of carbon atoms between two side carboxylate groups should be three. However, in our study, glutarate, with three carbon atoms in between two side carboxylate groups, can only produce silver nanoplates with a

Table 1. Carboxyl Compounds with Different Numbers of Carboxylate Groups and Chain Lengths That Have Been Used As the Capping Agent to Prepare Silver Nanoplates

Name	Structure	Number of carboxylate groups	Number of carbon between two nearest carboxylate groups	Yield of nanoplates
Acetate		1	N/A	~0%
Oxalate		2	0	~0%
Malonate		2	1	~80%
Succinate		2	2	~100%
Citramalate		2	2	~100%
Tartrate		2	2	~80%
Glutarate		2	3	~50%
Adipate		2	4	~20%
Pimelate		2	5	~0%
Citrate		3	2	~100%
Isocitrate		3	2	~90%
cis-Aconate		3	2	~90%
Tricarballylate		3	2	~85%
Trimesic Acid Trisodium Salt		3	3	~0%

yield around 50%. If we consider the two nearest carboxylate groups of citrate, the number of carbon atoms between each group is two, which is in great agreement with the cases of succinate and citramalate. We therefore suggest that the preferential binding of citrate to silver may come from the two nearest carboxylate groups rather than two side carboxylate groups. This was further confirmed by using tricarboxyl compounds as the capping agent. As listed in Table 1, *cis*-aconate, tricarballylate, and isocitrate can all be used to prepare silver nanoplates with relatively high yield (85–90%). In the case of trimesic acid, the low yield may come from its very low solubility in water, which prevents a sufficient supply of capping agent for surface protection. Although more advanced analyzing tools are still needed to probe the face-selective binding, it is now clear that citrate is not a “magic” ligand that leads to the formation of silver nanoplates; rather, it can be replaced by many other compounds containing dicarboxylate groups with proper molecular structures. It should be noted that a comprehensive computation by considering the 3D molecular structures of such carboxylate compounds (Supporting Information) and their interaction with the silver surface should be carried out in order to describe the origin of facet-selective binding more precisely.³⁷

Unlike many prior reports in which a secondary ligand, typically PVP, is needed for the growth of silver nanoplates, we have found that citrate ions alone can stabilize the silver nanoplates in addition to their face-selective protection property. In contrast to Mirkin and co-workers’ study in which only ill-defined particle aggregates could be formed without PVP or a

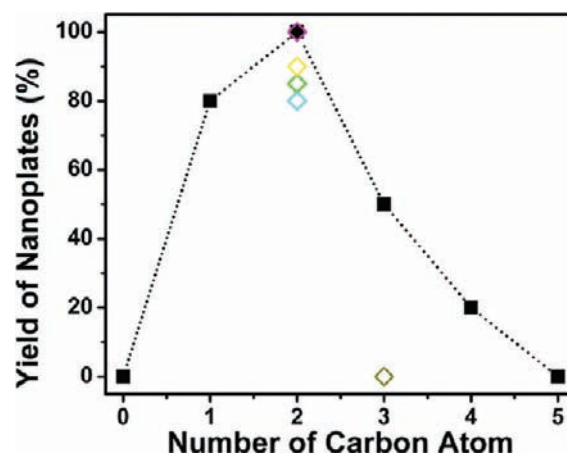


Figure 4. Yield of silver nanoplates as a function of the number of carbon atoms between two nearest carboxylate groups when carboxyl compounds are used as the capping agent.

similarly strong surfactant, BSPP (bis(*p*-sulfonatophenyl)phenylphosphine dihydrate dipotassium), we find that there is a narrow window of synthetic conditions in which citrate can stabilize the as-obtained silver nanoplates without the help of other ligands. When the concentration of H₂O₂ was 20 mM, silver nanoplates could be obtained with high yield (Figure 2a). However, due to the presence of excess H₂O₂, the as-obtained plates are not stable and will disappear within several hours. Reducing the concentration of H₂O₂ down to 10 mM yielded stable and well-defined triangular nanoplates with a yield of ~100%, as shown in Figures 5a and 5b. The stabilizing effect may come from the adsorption of citrate on the plate surface, rendering it negatively charged and preventing aggregation. Additionally, in the absence of PVP, the initiation time of the reaction is drastically decreased from ~20–30 min to 2–3 min. In other words, PVP molecules can slow down the reaction, mainly owing to their adsorption onto the initial silver nuclei. The exclusion of PVP allows precise control of the SPR band position in a more reproducible manner, likely due to fewer disturbances over a shorter reaction time.

The advantage of having PVP in the reaction is the improvement of the size distribution of the nanoplates. Comparing the samples obtained with/without PVP (Figures 1d and 5b), although triangular silver nanoplates can be obtained in high yield in both cases, the size distribution of the product in the presence of PVP is narrower, suggesting the size limiting effect of PVP as a typical surfactant. This effect, however, is not exclusive to PVP. We found that many hydroxyl group-containing molecules can be added to the reaction and help improve the size distribution of nanoplates. As shown in d and e of Figure 5, in one example, colloidal silver nanoplates with various colors can be obtained in the presence of glycerol. The size distribution also appears narrower than those synthesized with citrate alone (Supporting Information). Compared to the results in the presence of PVP (Figure 5d), the addition of glycerol shows a similar effect in the synthesis of silver nanoplates, further confirming that PVP is not an essential component in this synthetic strategy. An additional benefit of using the hydroxyl group-containing molecules is the relatively higher stability of the nanoplates against oxidation/ripening, probably due to the reductive nature of the hydroxyl groups. We found many hydroxyl group-containing compounds,

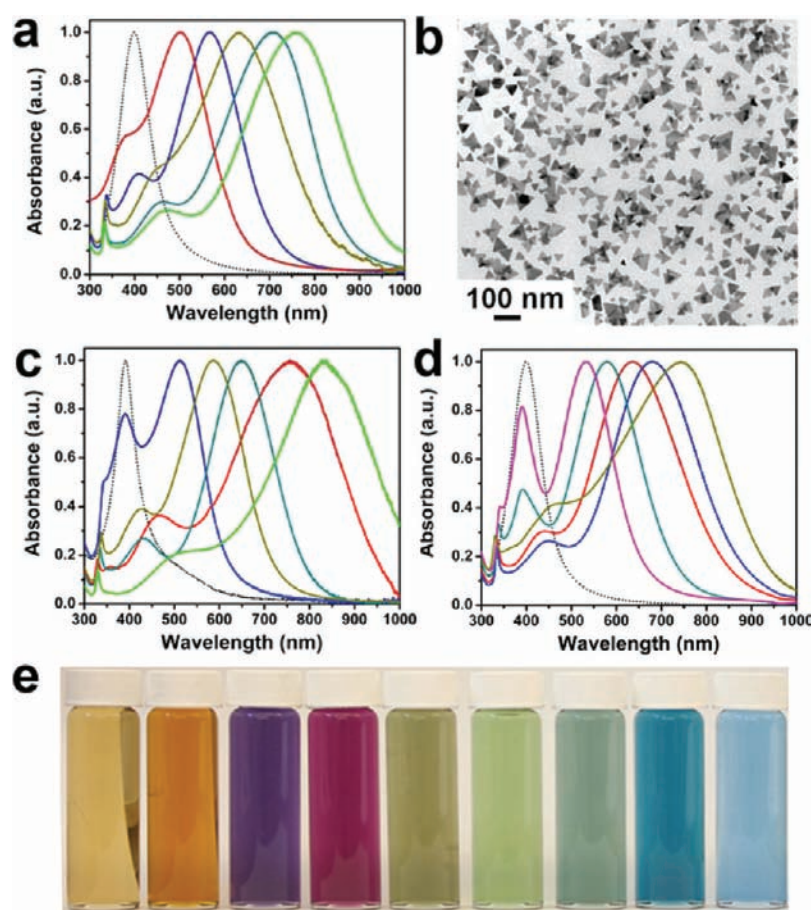


Figure 5. (a) UV/vis spectra and (b) TEM image showing the preparation of silver nanoplates by using citrate as the sole surfactant; (c) UV/vis spectra of Ag nanoplates prepared by using PVP as an additional stabilizing agent; (d, e) UV/vis spectra and digital image of silver nanoplates prepared in the presence of glycerol by tuning the synthetic conditions.

including ethanol, ethylene glycol (EG), diethylene glycol (DEG), tetraethylene glycol (TEG), polyethylene glycol (PEG) and polyvinyl alcohol (PVA), can be used in a similar manner to glycerol for synthesizing stable colloidal silver nanoplates with a high yield. Their enhanced stability against oxidation/ripening is supported by the small shift (<20 nm) of the plasmonic peak of the nanoplates upon storage in the reaction solution for one week, while control samples synthesized with citrate only or citrate/PVP in combination shifted ~ 150 and ~ 100 nm, respectively.

It has been widely accepted that NaBH_4 is a relatively strong reducing agent that can be used to reduce Ag^+ to Ag^0 . It is usually assumed that a higher concentration of NaBH_4 will lead to faster production of silver nanoparticles. However, our systematic studies show, for the first time, that borohydride ions can in fact slow down the nanoparticle formation by stabilizing the silver nanoparticles through surface binding. As a result, the initiation time required for nucleation increased with higher concentrations of NaBH_4 in the reaction system. The same trend has been observed for the reactions with or without ligands and H_2O_2 , as shown in Figure 6a. In particular, under typical reaction conditions but without any surfactant, the initiation time extended from several seconds to about 3 min with an increased concentration of NaBH_4 from 0.2 mM to 1.0 mM. The protecting effect of borohydride ions plays a very important role at this nucleation stage, which may come from the adsorption of borohydride ions

on silver nanoparticles so that the reaction rate is slowed down.⁴⁸ Likewise, the addition of citrate drastically delayed the reaction, as shown in Figure 6a. In the presence of citrate, the nucleation time increased from ~ 3 min to ~ 30 min when the concentration of NaBH_4 increased from 0.2 mM to 1.0 mM. The larger slopes of the cases involving citrate suggest a possible synergistic stabilizing effect of citrate ions and borohydride ions which, however, is difficult to fully interpret at this point.

The change of the nucleation kinetics can be used to effectively control both the thickness and aspect ratio of as-obtained silver nanoplates. As shown in Figure 6b, the thickness of silver nanoplates decreases from ~ 6 nm to ~ 3.5 nm as the concentration of NaBH_4 increases from 0.4 mM to 1.0 mM. This again supports the above assumption of a synergistic stabilizing effect between citrate ions and borohydride ions, where a higher concentration of borohydride ions enhances the preferential binding of citrate to the (111) facet, leading to the formation of thinner nanoplates. Likewise, the aspect ratio increases accordingly from ~ 3 to ~ 11 , which is consistent with the SPR band change (Supporting Information). We can thus conclude that NaBH_4 not only functions as a reducing agent but also works as a capping ligand that contributes to the reaction kinetics and morphology control. Interestingly, as a reducing agent, it does not play an essential role in the formation of silver nanoplates. For instance, we have been able to successfully produce silver nanoplates of considerably good quality by using ascorbic acid or

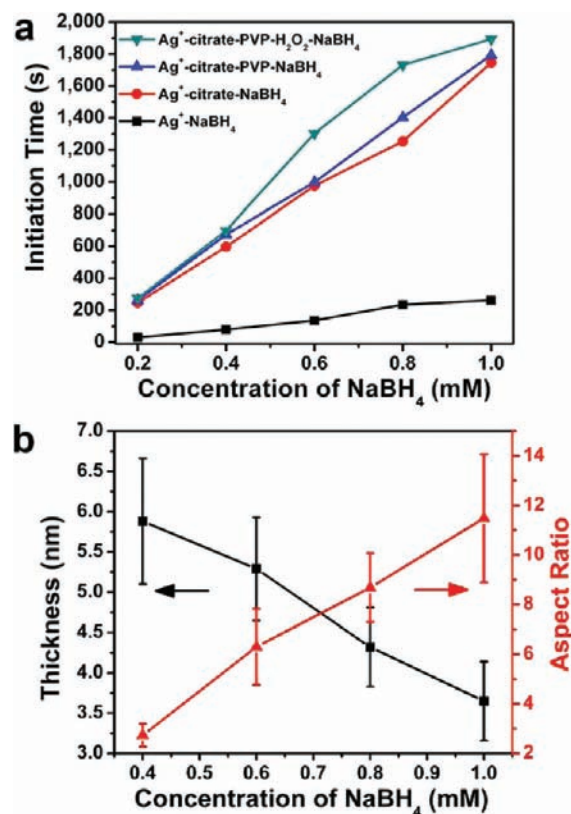


Figure 6. (a) Initiation time and (b) thickness and aspect ratio of as-obtained silver nanoplates as a function of the concentration of NaBH₄.

hydrazine in place of NaBH₄ as the reducing agent (Supporting Information).

CONCLUSION

We have carried out systematic studies and identified the specific roles of each reagent in the direct chemical reduction route to silver nanoplates. Contrary to the previous conclusion that citrate is the crucial component, we instead found that H₂O₂ plays an irreplaceable role in determining the shape evolution into plates. As a powerful oxidant, H₂O₂ favors the production of silver nanoplates by inducing the formation of planar twinned defects and removing other less stable structures. By harnessing the oxidative power of H₂O₂, various silver sources including metallic silver can now be directly converted to silver nanoplates with the assistance of an appropriate capping ligand, thus significantly enhancing the reproducibility of the nanoplate synthesis. We have also determined that the list of ligands with selective adhesion to Ag (111) facets can be expanded from citrate, which has been previously regarded as a “magic” irreplaceable ligand, to many di- and tricarboxylate compounds whose two nearest carboxylate groups are separated with two or three carbon atoms. In contrast to traditional practice, we found that a secondary capping ligand is not needed for preparing Ag nanoplates, although its presence may help to improve the size distribution of the product. In particular, the widely used secondary ligand PVP can be replaced by many hydroxyl group-containing compounds, which produce nanoplates of equal uniformity but superior stability against oxidation and ripening. In addition to the general understanding that NaBH₄ is a reducing agent, we found it also acts as a capping agent to stabilize the Ag nanoparticles as

evidenced by the prolonged initiation time required for nucleation at a higher concentration of NaBH₄. By tuning the nucleation kinetics through the concentration of NaBH₄, we are able to control the thickness as well as the aspect ratio of silver nanoplates. This work outlines the key components that determine the formation of Ag nanoplates, clarifies the roles of each reagent, provides highly reproducible recipes for synthesis, and therefore represents a significant step toward the complete understanding of the mechanism behind the experimental phenomena.

ASSOCIATED CONTENT

S Supporting Information. Experimental details; digital photos of nanoplate dispersion; additional TEM and SEM images and UV–vis spectra of the nanoplates; size distribution histograms, and video (avi) showing real-time spectra change during the nanoplate formation. This material is available free of charge via the Internet at <http://pubs.acs.org>.

AUTHOR INFORMATION

Corresponding Author

yadong.yin@ucr.edu

ACKNOWLEDGMENT

We thank the United States National Science Foundation (DMR-0956081), and Department of Energy (DE-SC0002247) for support of this research. Y.Y. also thanks the Research Corporation for Science Advancement for the Cottrell Scholar Award, 3M for the Nontenured Faculty Grant, and DuPont for the Young Professor Grant. N.L. acknowledges the fellowship support by the China Scholarship Council (CSC). We thank Dr. Qiang Fu in KTH Royal Institute of Technology (Sweden) for helpful discussion.

REFERENCES

- Pastoriza-Santos, I.; Liz-Marzan, L. M. *J. Mater. Chem.* **2008**, *18*, 1724.
- Millstone, J. E.; Hurst, S. J.; Metraux, G. S.; Cutler, J. L.; Mirkin, C. A. *Small* **2009**, *5*, 646.
- Mayer, K. M.; Hafner, J. H. *Chem. Rev.* **2011**, *111*, 3828.
- Jones, M. R.; Osberg, K. D.; Macfarlane, R. J.; Langille, M. R.; Mirkin, C. A. *Chem. Rev.* **2011**, *111*, 3736.
- Rycenga, M.; Cobley, C. M.; Zeng, J.; Li, W. Y.; Moran, C. H.; Zhang, Q.; Qin, D.; Xia, Y. N. *Chem. Rev.* **2011**, *111*, 3669.
- Kelly, K. L.; Coronado, E.; Zhao, L. L.; Schatz, G. C. *J. Phys. Chem. B* **2003**, *107*, 668.
- Jin, R. C.; Cao, Y. W.; Mirkin, C. A.; Kelly, K. L.; Schatz, G. C.; Zheng, J. G. *Science* **2001**, *294*, 1901.
- Jin, R. C.; Cao, Y. C.; Hao, E. C.; Metraux, G. S.; Schatz, G. C.; Mirkin, C. A. *Nature* **2003**, *425*, 487.
- Maillard, M.; Huang, P. R.; Brus, L. *Nano Lett.* **2003**, *3*, 1611.
- Xue, C.; Mirkin, C. A. *Angew. Chem., Int. Ed.* **2007**, *46*, 2036.
- Sun, Y. G.; Xia, Y. N. *Adv. Mater.* **2003**, *15*, 695.
- Xue, C.; Metraux, G. S.; Millstone, J. E.; Mirkin, C. A. *J. Am. Chem. Soc.* **2008**, *130*, 8337.
- Zhang, J.; Langille, M. R.; Mirkin, C. A. *J. Am. Chem. Soc.* **2010**, *132*, 12502.
- Chen, S. H.; Carroll, D. L. *Nano Lett.* **2002**, *2*, 1003.
- Sun, Y. G.; Mayers, B.; Xia, Y. N. *Nano Lett.* **2003**, *3*, 675.
- Xiong, Y.; Siekkinen, A. R.; Wang, J.; Yin, Y.; Kim, M. J.; Xia, Y. *J. Mater. Chem.* **2007**, *17*, 2600.
- Sun, Y. G.; Wiederrecht, G. P. *Small* **2007**, *3*, 1964.

- (18) Hao, E. C.; Kelly, K. L.; Hupp, J. T.; Schatz, G. C. *J. Am. Chem. Soc.* **2002**, *124*, 15182.
- (19) Jiang, L. P.; Xu, S.; Zhu, J. M.; Zhang, J. R.; Zhu, J. J.; Chen, H. Y. *Inorg. Chem.* **2004**, *43*, 5877.
- (20) Metraux, G. S.; Mirkin, C. A. *Adv. Mater.* **2005**, *17*, 412.
- (21) Zhang, Q.; Hu, Y.; Guo, S.; Goebel, J.; Yin, Y. *Nano Lett.* **2010**, *10*, 5037.
- (22) Jiang, X. C.; Chen, C. Y.; Chen, W. M.; Yu, A. B. *Langmuir* **2010**, *26*, 4400.
- (23) Zeng, J.; Tao, J.; Li, W.; Grant, J.; Zhu, Y.; Xia, Y. *Chem. Asian J.* **2011**, *6*, 376.
- (24) Zeng, J.; Xia, X.; Rycenga, M.; Henneghan, P.; Li, Q.; Xia, Y. *Angew. Chem., Int. Ed.* **2011**, *50*, 244.
- (25) Frank, A. J.; Cathcart, N.; Maly, K. E.; Kitaev, V. *J. Chem. Educ.* **2010**, *87*, 1098.
- (26) Wulff, G. Z. *Kristallogr.* **1901**, *34*, 449.
- (27) Elechiguerra, J. L.; Reyes-Gasga, J.; Yacamán, M. J. *J. Mater. Chem.* **2006**, *16*, 3906.
- (28) Leontidis, E.; Kleitou, K.; Kyprianidou-Leodidou, T.; Bekiari, V.; Lianos, P. *Langmuir* **2002**, *18*, 3659.
- (29) Tao, A. R.; Habas, S.; Yang, P. D. *Small* **2008**, *4*, 310.
- (30) Berriman, R. W.; Herz, R. H. *Nature* **1957**, *180*, 293.
- (31) Hamilton, D. R.; Seidensticker, R. G. *J. Appl. Phys.* **1960**, *31*, 1165.
- (32) Hosoya, Y.; Urabe, S. *J. Imaging Sci. Techn.* **1998**, *42*, 487.
- (33) Germain, V.; Li, J.; Inger, D.; Wang, Z. L.; Pileni, M. P. *J. Phys. Chem. B* **2003**, *107*, 8717.
- (34) Rocha, T. C. R.; Zanchet, D. *J. Phys. Chem. C* **2007**, *111*, 6989.
- (35) Aherne, D.; Ledwith, D. M.; Gara, M.; Kelly, J. M. *Adv. Funct. Mater.* **2008**, *18*, 2005.
- (36) Xia, Y.; Xiong, Y. J.; Lim, B.; Skrabalak, S. E. *Angew. Chem., Int. Ed.* **2009**, *48*, 60.
- (37) Kilin, D. S.; Prezhdo, O. V.; Xia, Y. *Chem. Phys. Lett.* **2008**, *458*, 113.
- (38) Zhang, Q.; Ge, J.; Pham, T.; Goebel, J.; Hu, Y.; Lu, Z.; Yin, Y. *Angew. Chem., Int. Ed.* **2009**, *48*, 3516.
- (39) Henglein, A. *Chem. Phys. Lett.* **1989**, *154*, 473.
- (40) Belloni, J.; Mostafavi, M.; Remita, H.; Marignier, J. L.; Delcourt, M. O. *New J. Chem.* **1998**, *22*, 1239.
- (41) Van Hynning, D. L.; Zukoski, C. F. *Langmuir* **1998**, *14*, 7034.
- (42) Mulvihill, M. J.; Ling, X. Y.; Henzie, J.; Yang, P. D. *J. Am. Chem. Soc.* **2010**, *132*, 268.
- (43) Hoare, J. P. *Standard Potentials in Aqueous Solution*; Marcel Dekker: New York, 1985.
- (44) Ho, C. M.; Yau, S. K.; Lok, C. N.; So, M. H.; Che, C. M. *Chem. Asian J.* **2010**, *5*, 285.
- (45) Millstone, J. E.; Metraux, G. S.; Mirkin, C. A. *Adv. Funct. Mater.* **2006**, *16*, 1209.
- (46) Ledwith, D. M.; Whelan, A. M.; Kelly, J. M. *J. Mater. Chem.* **2007**, *17*, 2459.
- (47) Mpourmpakis, G.; Vlachos, D. G. *Langmuir* **2008**, *24*, 7465.
- (48) Solomon, S. D.; Bahadory, M.; Jeyarajasingam, A. V.; Rutkowsky, S. A.; Boritz, C.; Mulfinger, L. *J. Chem. Educ.* **2007**, *84*, 322.